



## Species richness in North Atlantic fish: Process concealed by pattern

Gislason, Henrik; Collie, Jeremy; MacKenzie, Brian; Nielsen, Anders; Borges, Maria de Fátima; Bottari, Teresa; Chaves, Corina; Dolgov, Andrey V.; Dulčić, Jakov; Duplisea, Daniel

*Total number of authors:*  
30

*Published in:*  
Global Ecology and Biogeography

*Link to article, DOI:*  
[10.1111/geb.13068](https://doi.org/10.1111/geb.13068)

*Publication date:*  
2020

*Document Version*  
Peer reviewed version

[Link back to DTU Orbit](#)

### *Citation (APA):*

Gislason, H., Collie, J., MacKenzie, B., Nielsen, A., Borges, M. D. F., Bottari, T., Chaves, C., Dolgov, A. V., Dulčić, J., Duplisea, D., Fock, H. O., Gascuel, D., Gil de Sola, L., Hiddink, J. G., ter Hofstede, R., Isajlović, I., Jónasson, J. P., Jørgensen, O. A., Kristinsson, K., ... Vrgoč, N. (2020). Species richness in North Atlantic fish: Process concealed by pattern. *Global Ecology and Biogeography*, 29(5), 842-856.  
<https://doi.org/10.1111/geb.13068>

---

### General rights

Copyright and moral rights for the publications made accessible in the public portal are retained by the authors and/or other copyright owners and it is a condition of accessing publications that users recognise and abide by the legal requirements associated with these rights.

- Users may download and print one copy of any publication from the public portal for the purpose of private study or research.
- You may not further distribute the material or use it for any profit-making activity or commercial gain
- You may freely distribute the URL identifying the publication in the public portal

If you believe that this document breaches copyright please contact us providing details, and we will remove access to the work immediately and investigate your claim.

1 Species richness in North Atlantic fish: process concealed by pattern

2

3 Henrik Gislason<sup>1</sup>, Jeremy Collie<sup>2</sup>, Brian R. MacKenzie<sup>3</sup>, Anders Nielsen<sup>3</sup>, Maria de Fatima Borges<sup>4</sup>, Teresa  
4 Bottari<sup>5,6</sup>, Corina Chaves<sup>4</sup>, Andrey V. Dolgov<sup>7,8,9</sup>, Jakov Dulčić<sup>10</sup>, Daniel Duplisea<sup>11</sup>, Heino O. Fock<sup>12</sup>, Didier  
5 Gascuel<sup>13</sup>, Luís Gil de Sola<sup>14</sup>, Jan Geert Hiddink<sup>15</sup>, Remment ter Hofstede<sup>16</sup>, Igor Isajlović<sup>10</sup>, Jónas Páll Jonasson<sup>17</sup>,  
6 Ole Jørgensen<sup>3</sup>, Kristján Kristinsson<sup>17</sup>, Gudrun Marteinsdottir<sup>18</sup>, Hicham Masski<sup>19</sup>, Sanja Matić-Skoko<sup>10</sup>, Mark R.  
7 Payne<sup>3</sup>, Melita Peharda<sup>10</sup>, Jakup Reinert<sup>20</sup>, Jón Sólmundsson<sup>17</sup>, Cristina Silva<sup>4</sup>, Lilja Stefansdottir<sup>19</sup>, Francisco  
8 Velasco<sup>21</sup>, and Nedo Vrgoč<sup>10</sup>

9

10 <sup>1</sup>Corresponding author: DTU Aqua, Technical University of Denmark, Kemitovet, Building 202, DK2800 Lyngby,  
11 Denmark, E-mail:hg@aqua.dtu.dk, <sup>2</sup>Graduate School of Oceanography, University of Rhode Island,  
12 Narragansett, USA, <sup>3</sup>DTU Aqua, Technical University of Denmark, Kemitovet, Building 202, DK2800 Lyngby,  
13 Denmark, <sup>4</sup>Instituto Português do Mar e da Atmosfera (IPMA), Lisboa, Portugal, <sup>5</sup>Institute for Coastal Marine  
14 Environment (IAMC), National Research Council (CNR), Messina, Italy, <sup>6</sup>Stazione Zoologica Anton Dohrn, Centro  
15 Interdipartimentale della Sicilia, Italy, <sup>7</sup>Polar branch of Russian Federal Research Institute of Fisheries and  
16 Oceanography (PINRO named after N.M.Knipovich), Murmansk, Russia, <sup>8</sup>Murmansk State Technical University,  
17 Murmansk, Russia, <sup>9</sup>Tomsk State University, Tomsk, Russia, <sup>10</sup>Institute of Oceanography and Fisheries, Split,  
18 Croatia, <sup>11</sup>Fisheries and Oceans Canada, Institut Maurice-Lamontagne, Mont-Joli, QC, Canada, <sup>12</sup>Thuenen  
19 Institute of Sea Fisheries, Bremerhaven, Germany, <sup>13</sup>Agrocampus Ouest, Universite Europeenne de Bretagne,  
20 Rennes, cedex, France, <sup>14</sup>Instituto Español de Oceanografía, Málaga, Spain, <sup>15</sup>School of Ocean Sciences, Bangor  
21 University, Menai Bridge, Anglesey, UK, <sup>16</sup>Van Oord Dredging and Marine Contractors,  
22 Rotterdam, The Netherlands, <sup>17</sup>Marine and Freshwater Research Institute, Reykjavík, Iceland, <sup>18</sup>University of

23 Iceland, Reykjavik, Iceland, <sup>19</sup>Institut National de Recherche Halieutique, Casablanca, Morocco, <sup>20</sup>Faroe Marine

24 Research Institute, Tórshavn, Faroe Islands, <sup>21</sup>Instituto Español de Oceanografía, Santander, Spain.

25

26

27 Abstract

28 Aim

29 Previous analyses of marine fish species richness based on presence-absence data have shown  
30 changes with latitude and average species size, but little is known about the underlying processes. To  
31 elucidate these processes we use metabolic, neutral and descriptive statistical models to analyse how  
32 richness responds to maximum species length, fish abundance, temperature, primary production,  
33 depth, latitude, and longitude, while accounting for differences in species catchability, sampling effort  
34 and mesh size.

35 Data

36 Results from 53,382 bottom trawl hauls representing 50 fish assemblages.

37 Location

38 The northern Atlantic from Nova Scotia to Guinea.

39 Time period

40 1977-2013

41 Methods

42 A descriptive Generalised Additive Model was used to identify functional relationships between  
43 species richness and potential drivers, after which non-linear estimation techniques were used to

44 parameterize: 1) a 'best' fitting model of species richness built on the functional relationships, 2) an  
45 environmental model based on latitude, longitude and depth, and mechanistic models based on 3)  
46 metabolic and 4) neutral theory.

#### 47 Results

48 In the 'best' model the number of species observed is a lognormal function of maximum species  
49 length. It increases significantly with temperature, primary production, sampling effort and  
50 abundance, and declines with depth and, for small species, with the mesh size in the trawl. The 'best'  
51 model explains close to 90% of the deviance and the neutral, metabolic, and environmental models  
52 89%. In all four models, maximum species length and either temperature or latitude account for more  
53 than half of the deviance explained.

#### 54 Main conclusion

55 The two mechanistic models explain the patterns in demersal fish species richness in the northern  
56 Atlantic almost equally well. A better understanding of the underlying drivers is likely to require  
57 development of dynamic mechanistic models of richness and size evolution, fit not only to extant  
58 distributions, but also to historical environmental conditions and to past speciation and extinction  
59 rates.

60

61 Keywords: marine fish, biodiversity, species size, temperature, density, abundance.

62

63 Introduction

64

65 Although much has been learned about the richness and distribution of marine species, a mechanistic  
66 understanding of the processes responsible for generating and maintaining species richness over  
67 evolutionary timescales remains elusive. There is no generally accepted theory to explain the spatial  
68 distribution of marine species richness and no general understanding of why some species are more  
69 abundant than others (Fine, 2015). This lack of understanding is somewhat surprising. Strong  
70 latitudinal gradients in species richness are observed at global and regional scales and these often  
71 correlate significantly with environmental variables and life-history traits. Hillebrand (2004)  
72 conducted a meta-analysis of gradients in marine biodiversity and found significant relationships  
73 between marine species richness, latitude, and species size, while Tittensor et al. (2010) found water  
74 temperature to be the main environmental predictor of species richness across a number of marine  
75 taxonomic groups. Why latitude, temperature and species size are important is unclear, but size and  
76 maximum body size influence the trophic position, mortality, growth and reproduction of many  
77 marine species (Andersen et al., 2016), temperature affects their metabolism and food uptake  
78 (Gillooly, Brown, West, Savage & Charnov, 2001), and latitude determines the amplitude of the  
79 seasonal changes in solar energy input affecting primary production, average temperature and annual  
80 temperature range (Cullen, Franks, Karl & Longhurst, 2002).

81

82 Bony fish and elasmobranchs are among the best taxonomically resolved groups of marine animals  
83 and are therefore well suited for studies of marine species richness. Estimates suggest that on a

84 global scale around 79% of the species have now been described (Mora, Tittensor & Myers, 2008) and  
85 very few species have been declared extinct due to human activities (Davies & Baum, 2012). However,  
86 most inventories of fish species richness are based on single recordings of individuals with little  
87 consideration of differences in individual density and sampling effort. Including density and sampling  
88 effort is important for at least two reasons. The number of species recorded is known to depend  
89 statistically on the number of individuals and number of samples examined (Gotelli & Colwell, 2001),  
90 and high-density areas may have higher species richness because they harbor more individuals able to  
91 maintain a higher number of viable populations (Brown, 2014). Based on species inventories,  
92 MacPherson & Duarte (1994) found fish species richness and average maximum fish species size to  
93 increase with depth and decline with latitude in the northern Atlantic and Fisher, Franks & Leggett  
94 (2010) found the geometric mean fish species size to co-vary with species richness. While Blowes,  
95 Belmaker & Chase (2017) found the latitudinal change in reef fish richness to scale with abundance,  
96 no one has so far analysed how species richness of marine fish found on soft or sandy bottoms is  
97 related to density or abundance on a basin-wide scale.

98

99 To understand how fish species richness in different fish communities is related to density or  
100 abundance, species length, and environmental conditions, we analyse an extensive dataset,  
101 generated by collating results from 31 standardised bottom trawl surveys from the continental  
102 shelves of the northern Atlantic and adjacent areas (Figure 1). Our analysis is based on 123 million  
103 individual demersal or benthopelagic fish caught in 53 thousand hauls taken within a total survey area  
104 of 3.1 million km<sup>2</sup>. Bottom trawl surveys are often stratified to account for spatial or depth related

105 differences in fish assemblage composition and density. We retain the stratification used in the  
106 surveys, correct for differences in catchability, and further stratify species into log maximum species  
107 length intervals. Using a Generalised Additive Model (GAM) to identify significant variables and  
108 relationships we construct a 'best' descriptive model of the number of species caught per log  
109 maximum species length interval and survey stratum by transforming the significant relationships  
110 identified by the GAM into functional relationships. We also fit an environmental model to the data in  
111 which latitude, longitude, depth, total catch and mesh-size are used as independent variables without  
112 invoking any biological hypotheses. Using the two descriptive models as reference points we  
113 investigate how well mechanistic equilibrium models of species richness based on metabolic (Allen,  
114 Brown & Gillooly, 2002; Allen & Gillooly, 2007) and neutral theory (Hubbell, 2001) fit the survey data.  
115 Both theories explain the present difference in species richness among fish communities from  
116 individual density or abundance, and from fundamental evolutionary processes such as speciation,  
117 dispersal and extinction. Recently, they have been combined and used to simulate the latitudinal  
118 gradient in species richness in the ocean (Tittensor & Worm, 2016; Worm & Tittensor, 2018).

119

120 In brief, the basic assumption of metabolic theory is that temperature enhances species richness by  
121 increasing mutation rates and reducing generation times, while extinction rates are inversely related  
122 to the average density per species. In contrast to metabolic theory, neutral theory includes a spatial  
123 component and assumes that richness is determined by local abundance and random extinctions  
124 among functionally equivalent species counterbalanced by immigration from a surrounding meta-  
125 community where speciation takes place. Functionally equivalent species are defined as species that

126 share the same probabilities of death and reproduction (see Appendix S1 in Supporting Information  
127 for further information on the two models). Because natural mortality and reproductive output  
128 depend on body size in fish, we follow Reuman, Gislason, Barnes, Mélin & Jennings (2014) and  
129 assume that functional equivalence, primarily applies for species of similar maximum length. We  
130 therefore treat each maximum species length group separately. Comparing the results from the  
131 neutral and metabolic models with the two descriptive models, our aim is to elucidate the  
132 mechanisms behind the richness differences we observe across fish communities in the northern  
133 Atlantic.

134

## 135 Methods

136

### 137 Survey data

138 Average catch in number of individuals per species and haul was provided from 31 scientific bottom  
139 trawl surveys. The time period from which data was obtained from each survey was selected to  
140 provide temporal overlap between the surveys and as long a time period from each survey as feasible  
141 to minimise the influence of random fluctuations in recruitment and population abundance. Surveys  
142 with less than eight years of data were hence excluded. Although the earliest trawl hauls were taken  
143 in 1977 and the most recent in 2013, the period from 2001 to 2006 was covered by all surveys.  
144 Slightly more than half of the surveys took place in the period from October to March, a third in the  
145 period from April to September, and the remaining surveys included hauls obtained throughout the  
146 year (See Appendix S2 Table S2.1 in Supporting Information). Different bottom trawls were used in

147 the surveys. Cod-end mesh sizes ranged from 13 to 40 mm, horizontal trawl openings (wing spread)  
148 from 13 to 28 m, vertical openings from 1.9 to 7 m, and towing speeds from 3 to 4.5 knots. Many of  
149 the surveys used a stratified random sampling design to account for spatial and depth related  
150 differences in species composition. We retained the major strata used in the surveys, providing us  
151 with richness and density data from 50 different strata. The average depth in these strata ranged  
152 from 28 to 950 m.

153

154 Environmental data

155 Sea surface temperature, average temperature in the upper 200 m of the water column, and near  
156 bottom temperatures (Kelvin) were obtained from the World Ocean Atlas 2013 (Locarnini et al., 2013)  
157 based on decadal average temperature at 0.25° resolution covering the period 1955-2012 for annual,  
158 boreal summer (Jul-Sep) and boreal winter (Jan-Mar). Bottom temperatures were defined as the  
159 temperature in the layer closest to the bottom. Spatial averages were calculated for each survey  
160 stratum, and the seasonal amplitude calculated as the difference between summer and winter values.  
161 Estimates of depth integrated pelagic net primary production (npp,  $\text{gCm}^{-2}\text{y}^{-1}$ ) based on the satellite-  
162 derived Vertically Generalised Production Model (VGPM) (Behrenfeld & Falkowski, 1977) were  
163 downloaded from [www.science.oregonstate.edu/ocean.productivity](http://www.science.oregonstate.edu/ocean.productivity) at 1/12 degree monthly  
164 resolution for the period 2002-2012, from which estimates of mean annual npp were derived for each  
165 survey area. Latitude and longitude were calculated as the average of the minimum and maximum  
166 coordinates of each survey. Average depth was calculated as the midpoint of the depth range of each  
167 stratum (see Appendix S2 Table S2.1).

168

169 Fish species data

170 Among the fish taxa recorded some individuals had not been identified to species. If possible, we  
171 allocated these individuals to species, assuming that their relative species composition would be  
172 identical to that of the individuals identified within the same survey stratum, and family or genus.  
173 Where no species from the family or genus had been identified in a stratum, the family or genus  
174 name was retained. Information about the maximum length of each species was downloaded from  
175 FishBase (Froese & Pauly, 2016) and used to bin the observations into 11 log maximum length  
176 intervals of equal width (from now on denoted log maximum length groups). In 1% of the species  
177 records no maximum species length was available. These records were excluded from further  
178 calculations.

179

180 To estimate absolute fish density and abundance in a given stratum or area we first calculated swept  
181 area density for each species. This was done by dividing the average number of individuals caught per  
182 haul by the average area swept per haul, estimated by multiplying the wing spread of the trawl by the  
183 average distance covered per haul. Swept area abundance was calculated by multiplying swept area  
184 density by the size of the survey area. Swept area density and abundance can be converted to  
185 absolute density and abundance if catchability is known. Catchability, the fraction of the population in  
186 the path of the trawl that is retained and caught by the gear, can be estimated by dividing the swept  
187 area estimate of abundance by the absolute abundance provided by a stock assessment. Catchability  
188 is likely to differ between areas and species and depends on a number of factors including the

189 properties of the trawl and species-dependent traits such as the size, behavior and distribution of the  
190 individuals (Arreguín-Sánchez, 1996; Walker, Maxwell, Le Quesne & Jennings, 2017). To account for  
191 differences in horizontal and vertical distribution we sorted the species into: 1) species whose main  
192 distribution is outside the main depth range of the surveys (species mainly occurring in the infra-  
193 littoral zone and bathy-demersal or bathy-pelagic species found mainly at more than 200 m of depth),  
194 and species whose main distribution is inside the main depth range of the surveys, but either 2)  
195 mostly occur on either untrawlable grounds (species that are mainly found associated with reefs or in  
196 rocky areas), 3) are likely to have a low catchability (species that bury in the sediment, and pelagic  
197 species), or 4) are likely to be regularly retained by the survey gear when available (species resting on  
198 the seabed, species found close to but not on the seabed, and midwater species with some bottom  
199 contact).

200

201 We were able to identify 56 cases where catchability could be derived for the species, time period,  
202 and area covered by the survey data (see Appendix S3 and Table S3.1 in the Supporting Information).  
203 No catchability estimates could be derived for bathy-pelagic and bathy-demersal stocks, and few  
204 estimates could be obtained for infra-littoral species, for species mainly found associated with reefs  
205 or in rocky areas, and for burying and pelagic species; species that are likely to be under-sampled by  
206 the trawl surveys. The average catchability of these species was only 0.05, while the average  
207 catchabilities of the species in group four were 0.34, 1.04 and 0.52 for species that were resting on  
208 the seabed, found close to the seabed, or found in midwater, respectively. Note that for some of the  
209 species found close to the seabed the estimated catchability exceeded 1.0, probably due to their

210 response to the herding effect of the bridles, sweeps and doors of the trawl. Due to the few and low  
211 catchability estimates available for groups two and three, we decided to use only species from group  
212 four in our analysis. To extrapolate the 41 catchability estimates available for the 412 species in this  
213 group we fitted a log-linear mixed model to the estimates, using the vertical position of the species  
214 (resting on seabed, found close to but above the seabed, or midwater with some bottom contact) as a  
215 fixed variable and species identity and survey area as random factors. Drawing samples at random  
216 from the resulting stochastic model we generated 1000 estimates of catchability for each  
217 combination of species and survey stratum (see Appendix S3). The catchabilities were used to  
218 calculate average absolute density and abundance in each survey stratum for each of the species  
219 found in the surveys. Average absolute density and abundance were finally cumulated across species  
220 within each log maximum length group and survey stratum producing 550 data points as input to the  
221 models.

222

223 To confirm that the richness of the species in group four had been reasonably well sampled by the  
224 surveys we furthermore used the vegan package (Oksanen et al., 2019) to estimate the number of  
225 unobserved species in each survey stratum and found that on average a minimum of 7-8% of the  
226 species in a particular stratum may not have been recorded. However, considering all of the species  
227 found across the surveys few species appear to have been missed (see Appendix S4, Table S4.1 in  
228 Supporting Information).

229

230 Selection of independent variables

231 The number of species recorded in a survey stratum depends on the species richness in the stratum  
232 and the bias introduced by the sampling method. Using a bottom trawl to sample species richness is  
233 likely to generate a biased estimate of species richness because the number of species recorded  
234 depends on the number of individuals caught and identified (the species accumulation curve); the  
235 total area swept by the trawl (a measure of sampling effort); the vertical opening of the trawl  
236 (potentially influencing the catch of individuals and species trying to escape over the trawl); and its  
237 mesh-size (influencing the proportion of small individuals and species recorded in the catch). To  
238 account for the bias we included all four variables in the GAM model. We used the total area swept in  
239 each survey stratum rather than the total number of hauls to represent sampling effort because the  
240 average duration of the trawl hauls ranged from 15 minutes to one hour across surveys.

241

242 According to the metabolic and neutral models, richness should depend on temperature, species size,  
243 and either density or absolute abundance, but the size of the stratum (the species area relationship),  
244 net primary production, annual temperature range, latitude, longitude, and depth may also be  
245 important co-variates. Temperature may influence richness by affecting fish metabolism, generation  
246 time and mutation rate, but vary seasonally depending on latitude and longitude and with depth.

247 Identifying the biologically relevant ambient temperature for a fish species is therefore difficult.

248 Average sea surface temperature may be relevant for the pelagic eggs and larvae, average bottom  
249 temperature describes the average ambient temperature encountered by the juveniles and adults at  
250 the depth where they are caught by the survey trawls, and average temperature in the upper 200 m  
251 of the water column may represent the average temperature encountered during the entire life cycle.

252

253 We furthermore found more than a third of the pairwise correlations of the potential independent  
254 variables to be significant (See Appendix S2 Figure S2.2). Sea surface temperature, bottom  
255 temperature and water column temperatures were highly significantly correlated with each other and  
256 with both latitude and longitude, while the seasonal temperature range in the upper 200 m of the  
257 water column was significantly correlated to the seasonal temperature ranges near the bottom and at  
258 the surface. Net primary production decreased with latitude and increased with temperature, with  
259 both correlations highly significant. The vertical opening of the gear was highly significantly correlated  
260 to both latitude and to all three temperatures, but not to longitude, reflecting that surveys in high  
261 latitudes generally use larger trawls with larger vertical openings than surveys in low latitudes. Total  
262 area swept and total stratum area were also highly significantly positively correlated, reflecting that  
263 more hauls typically had been taken in large survey strata than in small. Finally, both catch in  
264 numbers, average abundance and total swept area were significantly correlated.

265

266 Identifying functional relationships

267 To find the 'best' descriptive model we used a Generalised Additive Model (GAM; Wood, 2006) to  
268 identify the functional form and error structure of the relationship between the number of species  
269 caught per log maximum length group and the independent variables using the R-package mgcv ver.  
270 1.8.22. In the GAM the log of the expected mean number of species caught,  $\mu_{i,j}$ , in survey stratum  $i$ ,  
271 maximum length group  $j$ , was described using:

272

$$\log(\mu_{i,j}) = \alpha + s_1(temp\_range_i) + s_2(temp_i) + s_3(abundance_{i,j}) + s_4(depth_i) + s_5(npp_i) + s_6(asurv_i) + s_7(lml_j) + s_8(catch_{i,j}) + s_9(aswept_i) + s_{10}(vertop_i) + s_{11,j}(mesh_i)$$

275

276 where  $\alpha$  is a proportionality constant; suffix  $i$  and  $j$  signify survey stratum and maximum length  
 277 group, respectively,  $temp\_range_i$  is the intra-annual temperature range in the stratum (Kelvin);  
 278  $temp_i$  is temperature (Kelvin);  $abundance_{i,j}$  is the average absolute abundance of fish of maximum  
 279 length  $j$  in stratum  $i$ ;  $depth_i$  is depth (m);  $npp_i$  is annual net primary production ( $gC\ m^{-2}\ y^{-1}$ );  $asurv_i$   
 280 is the total stratum area ( $km^2$ );  $lml_j$  is midpoint of log maximum length group (cm);  $catch_{i,j}$  is the  
 281 total number of fish caught in stratum  $i$ , maximum length group  $j$  over the time period of the survey;  
 282  $aswept_i$  is area swept by the survey trawl ( $km^2$ );  $mesh_i$  is mesh-size (mm); and  $vertop_i$  is the  
 283 vertical opening of the trawl (m). The  $s_1, \dots, s_{10}$  are general spline smoothers, while  $s_{11,j}$  denotes that  
 284 for each log maximum length group,  $j$ , a separate spline smoother was applied to describe the effect  
 285 of mesh-size on the number of species caught. The  $temp_i$  and  $temp\_range_i$  variables were either sea  
 286 surface, average upper 200 m water column or bottom temperature or were replaced by latitude,  
 287  $lat_i$ , and longitude,  $lon_i$ , when the effect of geographic location was examined, and  $abundance_{i,j}$   
 288 was changed to  $density_{i,j}$  to examine which of the two would provide the best fit.

289

290 We used thin plate regression splines with a basis dimension of four as smoothers and a log link. To  
 291 account for the correlation between many of the independent variables, we analysed the effect of  
 292 including these in separate model versions using residual plots and estimates of concurvity (a non-  
 293 linear analogue of multi-collinearity) to select the best fitting parameter combinations, and AIC-values

294 to identify the most parsimonious model. Model terms were selected by backwards removal of  
295 insignificant variables, after which co-variables generating an estimated concavity larger than 0.80  
296 were sequentially removed to reduce variance inflation and avoid bias. Distributions of residuals were  
297 visually inspected for normality and plotted against each co-variate to reveal heteroscedasticity. We  
298 compared models with Poisson and negative binomial error distributions, and found the two to  
299 provide an almost equally good fit to the data based on AIC-values and comparisons of the observed  
300 and theoretically expected variance, where the importance of over-dispersion was assessed by  
301 dividing the sum of squared residuals by the sample size minus the number of parameters estimated  
302 (Hilbe, 2011). For the negative binomial model this produced a variance ratio of 0.94, confirming the  
303 appropriateness of a negative binomial assumption.

304

305 We simplified the GAM model and further reduced its AIC value by inserting the functional  
306 relationships indicated by the significant GAM smoothers (see Figure 3). To model the effect of  
307 temperature, we assumed that the relationship between species richness and temperature would  
308 follow the Arrhenius equation (Gillooly et al., 2001) and consequently used the inverse of  
309 temperature in the model. The functional relationships included logarithmic transformations of  
310 several of the other independent variables and the addition of a second-order polynomial to capture  
311 the change in log species richness with log maximum length. All log transformations used natural  
312 logarithms. Using log transformations meant either that zero observations had to be excluded, or that  
313 a small positive number had to be added to avoid having to calculate the log of zero. When zero  
314 individuals had been caught in a given stratum and log maximum length group, we therefore used the

315 inverse of the total area swept in the stratum to provide a tentative estimate of its maximum density  
 316 in the stratum. As evidenced by the residuals, this introduced a small bias in the fit (see Appendix S5,  
 317 Figure S5.3). Because the neutral model cannot easily be linearised, we used non-linear techniques to  
 318 estimate the parameters of the four models presented below. This also allowed us to retain the zeros  
 319 and removed the source of the bias in the linearised GAM model.

320

321 Best descriptive model

322 The significant independent variables in the linearised GAM model were used to construct a ‘best’  
 323 non-linear descriptive model of the number of species caught. The ‘best’ non-linear model followed  
 324 the simplified GAM equation and contained an Arrhenius expression where  $\beta_2$ , the ‘activation energy  
 325 of metabolism’ (Gillooly et al., 2001), was divided by average water column temperature (Kelvin)  
 326 multiplied by Boltzmanns constant,  $k$  ( $8.62 \times 10^{-5} \text{ eV K}^{-1}$ ). It also contained total abundance, depth,  
 327 annual net primary production, and a quadratic log maximum length term,  $\exp(lml_j + \beta_7 lml_j^2)$ , to  
 328 capture the unimodal relationship between species richness and log maximum length, as well as the  
 329 catch in numbers, the area swept by the trawl, and a mesh-size/log maximum length interaction to  
 330 account for sampling bias:

331

$$332 \mu_{i,j} = \alpha * \exp\left(\frac{-\beta_2}{k * temp_i}\right) * abundance_{i,j}^{\beta_3} * depth_i^{\beta_4} * npp_i^{\beta_5} * \exp(lml_j + \beta_7 lml_j^2) * \\ 333 catch_{i,j}^{\beta_8} * aswept_i^{\beta_9} * mesh_i^{\beta_{11,j}}$$

334

335 where  $\alpha$ , the proportionality constant, subsumes the combined effects of the standardisation of the  
336 Arrhenius expression to a reference temperature, and other pre-factors related to abundance, depth,  
337 net primary production, the maximum length term, catch in numbers, area swept and mesh-size.

338

339 Environmental model

340 The environmental model assumes that the number of species observed in survey stratum,  $i$ , log  
341 maximum length group,  $j$ , can be calculated from species richness, described by a simple function of  
342 latitude, longitude, depth and log maximum length, corrected for differences in catch in numbers,  
343 area swept and mesh-size:

344

$$345 \mu_{i,j} = \alpha * lat_i^{\beta_0} * lon_i^{\beta_1} * depth_i^{\beta_4} * \exp(lml_j + \beta_7 lml_j^2) * catch_{i,j}^{\beta_8} * aswept_i^{\beta_9} * mesh_i^{\beta_{11,j}}$$

346

347 Metabolic model

348 In the Metabolic Theory of Ecology, temperature and body size influence the rate of per capita  
349 speciation in the same way as they influence metabolism (Gillooly & Allen, 2007) (see Appendix S1).  
350 Combining absolute density with a per capita rate of speciation determined by maximum length and  
351 temperature provides the speciation rate. In the equilibrium situation, speciation is counterbalanced  
352 by extinction, assumed to decline linearly with the average density per species. We added the effect  
353 of differences in number of individuals caught, area swept and trawl mesh-size to the model of Segura  
354 et al. (2015) to describe the number of species caught:

355

356 
$$\mu_{i,j} = \alpha * \exp\left(\frac{-\beta_2}{k * temp_i}\right) * density_{i,j}^{\beta_3} * ml_j^{\beta_6} * catch_{i,j}^{\beta_8} * aswept_i^{\beta_9} * mesh_i^{\beta_{11,j}}$$

357

358 where  $\beta_2$  is the 'activation energy of metabolism' (Gillooly & Allen, 2007),  $k$  is Boltzmann's constant,  
359  $ml_j$  is the median maximum length of the species in log maximum length group  $j$ , and  $\alpha$ , the  
360 proportionality constant, accounts for the combined effects of the standardisation of the Arrhenius  
361 expression to a reference temperature, as well as other pre-factors related to the density term, and to  
362 the maximum length, catch in numbers, area swept and mesh-size terms.

363

364 Neutral model

365 According to the Neutral Theory of Biodiversity and Biogeography, the number of functionally  
366 equivalent species in a local community is determined by random extinctions caused by ecological  
367 drift, counterbalanced by immigration of species from a larger surrounding meta-community where  
368 random speciation takes place (Hubbell, 2001; Rosindell, Hubbell & Etienne, 2011) (see Appendix S1).

369

370 Following Reuman et al. (2014), we assume that species of similar log maximum length are  
371 functionally equivalent and model each log maximum length group separately, using the approximate  
372 formula derived by Etienne & Olff (2004) and Reuman et al. (2014) to describe the relative number of  
373 species in each survey stratum and log maximum length group. We also assume that the probability  
374 of immigration,  $\lambda$ , is independent of stratum area, but allow it to vary with log maximum length. To  
375 account for the effect of differences in the number of individuals examined, effort and sampling gear

376 on the number of species caught, we add number of individuals caught, total area swept and mesh-  
 377 size terms to the species richness model of Reuman et al. (2014) providing the following equation:

378

$$379 \mu_{i,j} \approx J_{M_j} * \left( \frac{v_i}{1 - v_i} \right) * \log \left[ 1 - \frac{\lambda_j \log(\lambda_j)}{1 - \lambda_j} * \left( \frac{abundance_{i,j}}{J_{M_j} * (v_i / (1 - v_i))} \right) \right] * catch_{i,j}^{\beta_8} * aswept_j^{\beta_9} *$$

$$380 mesh_i^{\beta_{11,j}}$$

381

382 Where  $J_{M_j}$  is absolute abundance in log maximum length group  $j$  in the meta-community,  
 383  $abundance_{i,j}$  is the absolute abundance of group  $j$  in the local community, and  $v_i$  is the per capita  
 384 speciation rate in area  $i$ . Note also that  $J_{M_j}$  and  $v_i$  are confounded in the  $J_{M_j}(v_i/(1 - v_i))$  term.

385 However, as the speciation rate is likely to be very small, the term can be approximated by the  
 386 fundamental biodiversity number,  $\theta_{i,j} = J_{M_j} v_i$  (Rosindell et al., 2011). Because fish evolution is  
 387 affected by temperature (Wright, Ross, Keeling, McBride & Gillman, 2011), we follow Tittensor &  
 388 Worm (2016) and make  $v_i$  temperature dependent by adding the Arrhenius equation. Finally, we  
 389 approximate the change in  $J_{M_j}$  with log maximum length by a quadratic term as found in the ‘best’  
 390 descriptive model and thus end up with:

391

$$392 J_{M_j} \left( \frac{v_{i,j}}{1 - v_{i,j}} \right) \approx \theta_{i,j} = \alpha * \exp(lml_j + \beta_7 lml_j^2) * \exp\left(\frac{-\beta_2}{k * temp_i}\right)$$

393

394 where  $\alpha$  again is an overall proportionality constant. Hence

395

396 
$$\mu_{i,j} = \theta_{ij} * \log \left[ 1 - \frac{\lambda_j \log(\lambda_j)}{1 - \lambda_j} * \frac{abundance_{i,j}}{\theta_{ij}} \right] * catch_{i,j}^{\beta_8} * aswept_j^{\beta_9} * mesh_i^{\beta_{11,j}}$$

397

398 where,  $j = 1 \dots 11$ , is log maximum length group,  $i$  is stratum, and  $abundance_{i,j}$  is the total number  
399 of individuals in stratum  $i$  group  $j$  estimated by multiplying the size of stratum  $i$  with the absolute  
400 density of fish in  $i$  belonging to log maximum length group  $j$ .

401

402 Estimating model parameters

403 We used the non-linear model fitting R-package TMB (Kristensen, Nielsen, Berg, Skaug & Bell, 2015) to  
404 estimate the parameters of the four non-linear models. Fitting each model to the number of species  
405 observed we removed any insignificant variables, except if they were important for the theoretical  
406 underpinning of a model. We visually inspected the Pearson residuals of each model for normality and  
407 plotted them against each co-variate to reveal potential heteroscedasticity. To compare the models  
408 we calculated AIC-values (Burnham & Anderson, 2002),  $R^2$  from observed and predicted number of  
409 species, and proportion of deviance explained. The latter was estimated by fixing the estimated scale  
410 parameter,  $\kappa$ , of the negative binomial distribution used in each of the models, comparing the  
411 difference in deviance between a saturated model (with one parameter for each of the 550  
412 observations) and the actual model, to the difference in deviance between a saturated model and a  
413 model with only one parameter (Cameron & Windmeijer, 1996). To also illustrate how much of the  
414 overall deviance each model term explained, we consecutively replaced each of the independent  
415 variables by its overall average and calculated the relative increase in the proportion of deviance  
416 explained when the observations were used instead of the average. Having identified the four most

417 parsimonious models we examined their sensitivity to the uncertainty in the abundance and density  
418 data by fitting them to the 1000 separate estimates of density and abundance obtained from the  
419 mixed effects catchability model, and calculated the mean and variance of the resulting parameter  
420 estimates. We plotted the proportion of the deviance explained by each of the model variables in the  
421 1000 runs, and used these to illustrate the sensitivity of our results to the uncertainty in the  
422 catchability estimates. All analyses were undertaken in R version 3.4.4.

423

424

425 Results

426

427 Observed number of species and density

428 The number of observed species, log average swept area density, and log average absolute density  
429 follow almost symmetrical distributions when plotted against log maximum length (Figure 2). As  
430 expected, the average number of species observed increases with temperature while log average  
431 swept area density and log average absolute density change little except in areas with a mean annual  
432 sea temperature below 7.5°C where the densities are significantly lower in the intermediate length  
433 range.

434

435 GAM model

436 Fitting the GAM to the survey data reveals a strong and highly significant unimodal effect of log  
437 maximum length on log number of species observed, a significant effect of absolute fish abundance,

438 significant non-linear positive effects of average temperature in the upper 200 m of the water column  
439 and area swept, and a significant positive linear effect of net primary production. Log number of  
440 species caught declined significantly with depth and, for the smaller length groups, with increasing  
441 mesh-size (Figure 3). Vertical opening, temperature range and catch in numbers were all insignificant,  
442 while stratum area was significant ( $p=0.02$ ), but generated a too high concavity to be retained due to  
443 its high correlation with area swept. The model explained 85% of the deviance and had a lower AIC  
444 than model versions in which abundance was replaced by density. Using average temperature  
445 produced a lower AIC than bottom temperature and latitude and longitude, and a slightly higher AIC  
446 than sea surface temperature, but the best variance ratio. Although there are survey strata that  
447 produce significant negative residuals, such as the 50-200m stratum in Guinea which features the  
448 lowest number of hauls of all strata, there are no clear patterns in the residuals across survey strata.  
449 This suggests that the model provides an equally good description of fish species richness in the  
450 Atlantic, Arctic and Mediterranean Seas (Figure 4). Further model diagnostics are shown in Appendix  
451 S5, Figures S5.1a&b and S5.2).

452

453 Some of the smooth relationships suggested that the AIC value could be further reduced by using the  
454 logarithm or the inverse of the independent variable, and for log maximum length, in particular, that  
455 the smoother could be replaced by a second-order term, corresponding to a log-normal like  
456 distribution of richness versus maximum length. Replacing the independent variables in the GAM by  
457 inverse temperature, log abundance, log depth, net primary production, log area swept, an  
458 interaction between mesh-size and log maximum length, and the exponential of a second-order

459 polynomial in log maximum length, reduced the AIC-value from 2090 to 1860 and increased the  
460 percentage of deviance explained to 91%.

461

462 Non-linear models

463 We use non-linear estimation techniques to compare the ‘best’ descriptive model identified by the

464 GAM to the three other models. Fitting the four models to the average absolute densities and

465 abundances we initially used variance ratio tests to determine whether the bias correcting terms

466 ( $catch_{i,j}^{\beta_8}$ ,  $aswept_j^{\beta_9}$  and  $mesh_i^{\beta_{11,j}}$ ) contributed significantly to the fit. We found that

467  $catch_{i,j}^{\beta_8}$  did not improve the fit of the ‘best’ and neutral models significantly, improved the

468 metabolic model marginally, but contributed highly significantly to the fit of the environmental

469 model. The total area swept,  $aswept_j^{\beta_9}$ , contributed significantly to all models, except the

470 environmental, while the term reflecting the interaction between mesh size and maximum length,

471  $mesh_i^{\beta_{11,j}}$ , was significant in all four models. In the neutral model the per capita immigration rates,  $\lambda_j$ ,

472 were not significantly different from zero; and were therefore replaced by a single overall  $\lambda$  for all log

473 maximum length groups (see Appendix S5 Table S5.1).

474

475 Fitting the ‘best’ model to the average of the absolute abundances explains 90% of the deviance

476 (Table 1). The neutral model provides the second-best fit ( $\Delta AIC=38$ ) followed by the metabolic model

477 ( $\Delta AIC=40$ ) and the environmental model ( $\Delta AIC=46$ ). Note that the difference between the metabolic

478 and neutral models can be explained by the additional parameter included in the former. Many of the

479 parameter estimates are similar across models. The interaction between log maximum length and

480 mesh-size,  $\beta_{11,j}$ , is thus negative for the smaller species in all models, implying a general decline in  
481 the number of small species caught as mesh-size increases. In all models log maximum length and  
482 either temperature or latitude account for most of the deviance explained (Figure 5). The parameter  
483 estimates of 'best', metabolic and neutral models are robust to the uncertainty in the modelled  
484 catchabilities as shown by the limited distribution of deviance around the mean value of the 1000  
485 estimates. The standard deviations of the parameter estimates are also small (see Appendix S5 Table  
486 S5.1). Additional model diagnostics are presented in the Supplementary Information (Appendix S5  
487 Figures S5.4 & S5.5).

488

489

490 Discussion

491

492 Our study reveals strong consistent patterns in the number of demersal and benthopelagic fish  
493 species across the northern Atlantic. As in previous investigations, we find body size, depth and either  
494 temperature or latitude to be important, but our analysis is the first in which differences in the  
495 number of individuals caught, area swept and mesh-size are considered, and where net primary  
496 production and absolute fish abundance or density are used as covariates. We find fish species  
497 richness to increase with temperature, fish abundance, and net primary production, but to decline  
498 with depth and latitude. Adjusting for differences in area swept and mesh-size, the 'best' descriptive  
499 model explains 90% of the deviance in the number of species caught by log maximum length,  
500 temperature, fish abundance, depth and primary production (Table 1). The neutral model in which

501 inverse temperature, a parabolic relationship with log maximum length, area swept and mesh-size are  
502 significant, explains 89% of the deviance, and so does the metabolic model. Our analyses furthermore  
503 show that both the neutral and metabolic models provide significantly better fits than the  
504 environmental model in which local richness is described as a function of log maximum length, catch,  
505 latitude, longitude and depth.

506

507 In all four non-linear models more than half of the deviance is explained by a combination of log  
508 maximum length and either temperature or latitude (Figure 5). In the data the distribution of the  
509 number of species observed across maximum length groups is approximately lognormal (Figure 2).  
510 Similar distributions have been obtained for marine bivalves (Roy, Jablonsky & Martien, 2000),  
511 terrestrial snakes (Boback & Guyer, 2003), and insects (Siemann, Tilman & Haarstad, 1996), while  
512 more right-skewed distributions have been found for birds and mammals (Purvis, Orme & Dolphin,  
513 2003; Smith & Lyons, 2013). A lognormal distribution also provided a highly significant fit in the best,  
514 neutral and environmental models (Table 1). Contrary to this, metabolic theory predicts that species  
515 richness should scale with body mass raised to a power of 0.75, hence maximum length to a power of  
516 2.25. This prediction was not confirmed by our analysis in which the power was estimated to be -1.00  
517 ( $\pm 0.48$  conf. lim.) and thus highly significantly different from the expected.

518

519 The average water column temperature from 0-200 m is only a marginally better predictor of the  
520 observed number of fish species than surface temperature, but much better than bottom  
521 temperature, and latitude and longitude. Latitude and average temperature are negatively correlated,

522 but the correlation breaks down at intermediate latitudes, where average temperature generally is  
523 higher in the eastern part of the northern Atlantic due to the influence of the Gulf Stream. The  
524 increase in the number of fish species caught with temperature seems to be well described by the  
525 Arrhenius equation. Metabolic theory emphasizes the role of temperature and body size on mutation  
526 rate and generation time, and it is interesting that the Arrhenius constant,  $\beta_2$ , is 0.47 ( $\pm 0.06$  conf.  
527 lim.) and 0.52 eV ( $\pm 0.06$  conf. lim.), respectively, in the metabolic and neutral models. This range is  
528 not far from the average activation energy of metabolism of 0.65 eV predicted by metabolic theory  
529 (Gillooly & Allen, 2007; Bailly et al., 2014), and close to empirical estimates of the activation energy of  
530 fish metabolism. Clarke & Johnston (1999) and Gillooly et al. (2001) both used the Arrhenius equation  
531 to describe the relationship between the resting metabolism of fish and temperature, and  
532 independently estimated the activation energy as 0.43 eV. Barneche et al. (2014) used a model with a  
533 temperature optimum to account for metabolic inactivation at high temperatures and found an  
534 activation energy of 0.59 eV. How temperature influences the rates of speciation and extinction is not  
535 completely known, and other co-varying factors may be involved (see e.g. Rabosky et al., 2018).

536

537 The 'best' and neutral models contain positive relationships between abundance and the number of  
538 species observed. The 'best' model also includes a significant positive relationship with net primary  
539 production. Areas of high productivity have been hypothesised to have higher species richness  
540 because they harbor more individuals able to maintain a higher number of viable populations (Brown,  
541 2014), although a recent review by Storch, Bodhalkvá & Okie (2018) found the empirical evidence in  
542 favor of this hypothesis to be mixed. However, in areas where abundance has been significantly

543 reduced by fishing, primary production may better reflect fish abundance and density in the  
544 unexploited state and hence be a better predictor of richness. Without primary production included in  
545 the model, the three largest positive differences between the observed and predicted number of  
546 species were generated by the data from the shelf off Mauretania, which features the highest primary  
547 production, but has been subject to marked overexploitation (Meissa & Gascuel, 2014). Note  
548 however, that abundance or density never accounted for more than 10% of the total deviance in the  
549 'best', neutral and metabolic models, explaining the robustness of these models to the uncertainty in  
550 the catchabilities (Figure 5).

551

552 Tittensor & Worm (2016) and Worm & Tittensor (2018) used a neutral model to simulate species  
553 richness in the ocean and allowed speciation rate and generation time to depend on temperature.  
554 Thermal effects on speciation rate generated a stable but weak latitudinal richness gradient in their  
555 model, while thermal effects on generation time produced a transient latitudinal richness gradient  
556 that eventually disappeared. Combining the effect of an increase in abundance caused by the increase  
557 in ocean area towards the equator and a temperature-dependent speciation rate produced the most  
558 realistic gradient in richness. Fitting a neutral model to the survey data we found a strong effect of  
559 temperature on species richness and a weaker influence of fish abundance. Furthermore, the shelf  
560 areas in the eastern Atlantic down to 200 m, the depth range where our fish species have their  
561 maximum abundance, increases with latitude from the Equator to the Arctic (Pilson & Seitzinger,  
562 1996). A consistent decline in habitat area with latitude is therefore unlikely to explain our results.

563

564 The parameter describing the probability of immigration in the neutral model could not be estimated  
565 with sufficient precision. The known functional dependency between per capita immigration  
566 probability and the speciation rate in the surrounding meta-community makes it difficult to estimate  
567 both parameters simultaneously (Jabot & Chave, 2011). The immigration probability may depend on  
568 temperature and size, as assumed by Reuman et al. (2014), but the evidence for temperature related  
569 differences in larval dispersal is lacking (Leis et al., 2013), and when immigration probability was  
570 assumed to be size dependent, none of the estimates of  $\lambda_j$  were significant. Additional analysis of  
571 species distributions and information on the genetic divergence of subpopulations is necessary to  
572 fully understand the relationship. The neutral model has been criticised for predicting unrealistically  
573 long species ages for common species and too short species ages for new species with few individuals  
574 (Chisholm & O'Dwyer, 2014). Recent work has shown that more realistic species ages are generated  
575 when protracted speciation and weak selection caused by small differences in hereditary fitness are  
576 incorporated in the model (Rosindell et al., 2015), but no approximate solution for the number of  
577 species in each community is yet available for this model.

578

579 Despite the large sample sizes and good geographical coverage of the survey data, several problems  
580 may be associated with using bottom trawl survey data to study fish species richness and density  
581 patterns. The main aim of a scientific bottom trawl survey is often to provide reliable estimates of the  
582 relative abundance and year-class strength of commercially important fish species, and less attention  
583 may therefore be given to identifying species that are rare or of little or no commercial value. Trawl-  
584 survey catches may furthermore provide biased estimates of the species composition and density due

585 to species and size-specific differences in the probability of the individuals being retained by the trawl  
586 (Arreguín-Sánchez, 1996). Some species and sizes are herded into the path of the trawl by the action  
587 of the otter doors and trawl sweeps, others escape under the fishing line or over the headline, while  
588 yet others are able to outswim the trawl. Among those entering the trawl the smaller individuals and  
589 species may escape through the meshes. Factors that have been reported to influence the catch  
590 efficiency of survey trawls include time of day, light intensity, turbidity, current strength and  
591 direction, depth, sweep length, net spread, vertical opening, trawl speed, haul duration, and the size  
592 and type of the ground gear (Arreguín-Sánchez, 1996; Fraser, Greenstreet & Piet, 2007). Although we  
593 corrected our analysis for differences in species catchability, we were unable to fully account for all of  
594 the factors that may lead to species and size specific differences in catchability. This was due to the  
595 sparsity of spatially and temporally overlapping stock assessments, the absence of individual length  
596 measurements for many of the non-commercial species, and our use of average catch rates rather  
597 than individual hauls. However, as seen in Figure 5, density or abundance only explains less than 10%  
598 of the deviance. The sensitivity of our overall conclusions to the uncertainty in the catchabilities is  
599 therefore modest, and the parameter estimates and the relative importance of the variables change  
600 little in the different models. Finally, our use of a single estimate of maximum length for each species  
601 hides the fact that maximum body length in fish is likely to vary from area to area (Rypel, 2013).  
602 However, the maximum length of a species in a given area is difficult to estimate as it depends on  
603 local fishing mortality and sampling effort.

604

605 We base our analysis on the number of fish species and individuals observed over a recent period of  
606 time in different regions of the northern Atlantic, Arctic and Mediterranean Seas. It is now well  
607 documented that changes in fish distributions have occurred over the last decade or two in many  
608 regions of the North Atlantic and that these are significantly associated with changes in temperature,  
609 (Perry, Low, Ellis & Reynolds, 2005; Hiddink & Ter Hofstede, 2008; Fossheim et al., 2015; Batt,  
610 Morley, Selden, Tingley & Pinsky, 2017). We have fitted our models to data from a period when  
611 temperatures have been increasing, but where regulatory processes generally seem to maintain  
612 existing patterns in species richness (Gotelli et al., 2017). Future analyses should investigate whether  
613 these patterns will persist over longer time periods and how our model parameters will be modified  
614 by temperature change, for example by conducting the analyses on different time periods  
615 characterised by different mean temperatures. Such analyses could provide insight into the relative  
616 importance of temperature having a direct effect on metabolic processes vs. its effects on other  
617 ecosystem features that affect species richness. For example, Marbá, Jordà, Augustí, Girard & Duarte  
618 (2015) showed that the activation energy for many biological responses in the Mediterranean Sea is  
619 far higher than the reported activation energy for metabolism, suggesting that temperature increases  
620 are having additional ecosystem effects on biotic responses beyond their effect on metabolic  
621 processes and speciation rates. The effects of global warming on fish communities have been  
622 predicted from stacked species distribution models (SSDMs; e.g. Jones & Cheung, 2015), but these  
623 models have so far largely ignored the regularity in the distribution of fish species richness and  
624 abundance with log maximum length. This regularity accounts for a third or more of the deviance  
625 explained by our models (Figure 5) and may thus be used to improve the predictive capability of the

626 SSDMs significantly. But while the right-hand side of the richness versus log maximum length  
627 distribution, consisting of species with a maximum length larger than app. 50 cm, has been explained  
628 by size spectrum theory (Reuman et al., 2014), little is known about the processes shaping the left-  
629 hand side.

630

631 Numerous hypotheses have been put forward to explain the latitudinal pattern in species richness  
632 (Brown, 2014; Fine, 2015). Finding log maximum length, temperature, absolute fish abundance, depth  
633 and net primary production to explain 90% of the deviance in the distribution of demersal fish species  
634 richness across the northern Atlantic, and both neutral and metabolic equilibrium models to explain  
635 close to 89%, conveys an important message. When 89% of the deviance in the extant species  
636 richness can be explained by two competing mechanistic hypotheses, and by a model based on  
637 latitude, longitude and depth, and when many of the independent variables are significantly  
638 correlated, it seems relevant to question how much the present patterns in species richness and  
639 abundance can tell us about the underlying environmental, ecological and evolutionary processes  
640 (Gotelli et al., 2009). We probably need dynamic mechanistic models with more realistic descriptions  
641 of speciation, dispersal and extinction plus additional data to reveal how past changes in  
642 environmental (e.g. temperature, currents, ice cover, shelf area) and biotic (e.g. primary production)  
643 variables may have contributed to shaping the present distribution of species richness and the strong  
644 lognormal relationship between richness and maximum length (Fine, 2015; Descombes et al., 2018).  
645 Such data should include information from paleo-geographical and climatological reconstructions of  
646 past environmental conditions as well as information about body size evolution, diversification rates

647 and species lifetimes from molecular phylogenetics and the fossil record (Romano et al., 2016; Alfaro  
648 et al., 2018). In addition to providing a baseline from which we can evaluate future change, our data  
649 and results point to new possibilities for understanding demersal fish species biogeography in the  
650 northern Atlantic.

651

## 652 Acknowledgements

653 Thanks to all the scientists and crew members engaged in the Scientific Trawl Surveys that provided  
654 the data for this paper. Thanks also to E. Collie and four anonymous referees for suggesting  
655 improvements to the manuscript. Initial data compilations from EU waters were conducted as part of  
656 the EU Network of Excellence MarBEF (Marine Biodiversity and Ecosystem Functioning; contract  
657 number GOCE-CT-2003-505446), and supported by the Center for Macroecology, Evolution and  
658 Climate (Danish National Research Foundation). The first author received support from the EU FP7-  
659 KBBE project VECTORS (project ID: 266445).

660

661 References

- 662 Alfaro, M.E., Faircloth, B.C., Harrington, R.C., Sorenson, L., Friedman, M., Thacker, ... Near, T.J., 2018.  
663 Explosive diversification of marine fishes at the Cretaceous-Palaeogene boundary. *Nature*  
664 *Ecology and Evolution*, 2, 688-696.
- 665 Allen, A.P., Brown, J.H. & Gillooly, J.F., 2002. Global biodiversity, biochemical kinetics, and the  
666 energetic-equivalence rule. *Science*, 297, 1545-1548.
- 667 Allen, A.P., & Gillooly, J.F., 2007. The mechanistic basis of the metabolic theory of ecology. *Oikos*,  
668 116, 1073-1077.
- 669 Andersen, K.H., Berge, T., Gonçalves, R.J., Hartvig, M., Heuschele, J., Hylander, S., ... Olsson, K., 2016.  
670 Characteristic sizes of life in the oceans, from bacteria to whales. *Annual Review of Marine*  
671 *Science*, 8, 217-241.
- 672 Arreguín-Sánchez, F., 1996. Catchability: a key parameter for fish stock assessment. *Reviews in Fish*  
673 *Biology and Fisheries*, 6, 221-242.
- 674 Bailly, D., Cassemiro, F.A., Agostinho, C.S., Marques, E.E. & Agostinho, A.A., 2014. The metabolic  
675 theory of ecology convincingly explains the latitudinal diversity gradient of Neotropical  
676 freshwater fish. *Ecology*, 95, 553-562.
- 677 Barneche, D.R, Kulbicki, M., Floeter, S.R., Friedlander, A.M., Maina, J., & Allen, A.P., 2014. Scaling  
678 metabolism from individuals to reef-fish communities at broad spatial scales. *Ecology Letters*,  
679 17, 1067-1076.
- 680 Batt, R.D., Morley, J.W., Selden, R.L., Tingley, M.W. & Pinsky, M.L., 2017. Gradual changes in range  
681 size accompany long-term trends in species richness. *Ecology Letters*, 20, pp.1148-1157.

682 Behrenfeld, M.J. & Falkowski, P.G., 1977. Photosynthetic rates derived from satellite-based  
683 chlorophyll concentration. *Limnology and Oceanography*, 42, 1-20.

684 Blowes, S. A., Belmaker, J. & Chase, J. M., 2017. Global reef fish richness gradients emerge from  
685 divergent and scale-dependent component changes. *Proceedings of the Royal Society B:*  
686 *Biological Sciences*, 284, 20170947.

687 Boback, S.M., & Guyer, C., 2003. Empirical evidence for an optimal body size in snakes. *Evolution*,  
688 57, 345-351.

689 Brown, J. H., 2014. Why are there so many species in the tropics? *Journal of Biogeography*, 41, 8-22.

690 Burnham, K.P., & Anderson, D. R., 2002. *Model selection and multimodel inference: a practical*  
691 *information theoretic approach*. 2nd ed. Springer, New York, 488pp.

692 Cameron, A.C. & Windmeijer, F.A., 1996. R-squared measures for count data regression models with  
693 applications to health-care utilization. *Journal of Business and Economic Statistics*, 14, 209-220.

694 Chisholm, R.A. & O'Dwyer, J.P., 2014. Species ages in neutral biodiversity models. *Theoretical*  
695 *Population Biology*, 93, 85-94.

696 Clarke, A., & Johnston, N.M., 1999. Scaling of metabolic rate with body mass and temperature in  
697 teleost fish. *Journal of Animal Ecology*, 68, 893-905.

698 Cullen, J. J., Franks, P. J., Karl, D. M., & Longhurst, A., 2002. Physical influences on marine ecosystem  
699 dynamics. In Robinson A.R., McCarthy, J.J. & Rothschild, B.J. (eds.). *The Sea*, 12, 297-336.

700 Davies, T.D. & Baum, J.K., 2012. Extinction risk and overfishing: reconciling conservation and  
701 fisheries perspectives on the status of marine fishes. *Scientific reports*, 2, p.561.

702 Descombes, P., Gaboriau, T., Albouy, C., Heine, C., Leprieur, F., & Pellissier, L., 2018. Linking species  
703 diversification to palaeo-environmental changes: A process-based modelling approach. *Global*  
704 *Ecology and Biogeography*, 27, 233-244.

705 Etienne, R.S., & Olff, H., 2004. How dispersal limitation shapes species body size distributions in local  
706 communities. *The American Naturalist*, 163, 69-83.

707 Fine, P.V., 2015. Ecological and evolutionary drivers of geographic variation in species diversity.  
708 *Annual Review of Ecology, Evolution, and Systematics*, 46, 369-392.

709 Fisher, J.A., Frank, K.T., & Leggett, W.C., 2010. Global variation in marine fish body size and its role in  
710 biodiversity–ecosystem functioning. *Marine Ecology Progress Series*, 405, 1-13.

711 Fossheim, M., Primicerio, R., Johannesen, E., Ingvaldsen, R.B., Aschan, M.M., & Dolgov, A.V., 2015.  
712 Recent warming leads to a rapid borealization of fish communities in the Arctic. *Nature Climate*  
713 *Change*, 5, 673–677.

714 Fraser, H.M., Greenstreet, S.P. and Piet, G.J., 2007. Taking account of catchability in groundfish  
715 survey trawls: implications for estimating demersal fish biomass. *ICES Journal of Marine*  
716 *Science*, 64, 1800-1819.

717 Froese, R., & Pauly, D., (eds.), 2016. FishBase. World Wide Web electronic publication.  
718 [www.fishbase.org](http://www.fishbase.org), version (01/2016).

719 Gillooly, J.F., Brown, J.H., West, G.B., Savage, V.M., & Charnov, E.L., 2001. Effects of size and  
720 temperature on metabolic rate. *Science*, 293, 2248-2251.

721 Gillooly, J.F., & Allen, A.P., 2007. Linking global patterns in biodiversity to evolutionary dynamics  
722 using metabolic theory. *Ecology*, 88, 1890-1894.

723 Gotelli, N.J., Anderson, M.J., Arita, H.T., Chao, A., Colwell, R.K., Connolly, S.R., ... Willig, M.R., 2009.  
724 Patterns and causes of species richness: a general simulation model for macroecology. *Ecology*  
725 *Letters*, 12, 873-886.

726 Gotelli, N. J., & Colwell, R. K., 2001. Quantifying biodiversity: procedures and pitfalls in the  
727 measurement and comparison of species richness. *Ecology Letters*, 4, 379-391.

728 Gotelli, N.J., Shimadzu, H., Dornelas, M., McGill, B., Moyes, F., & Magurran, A.E., 2017. Community-  
729 level regulation of temporal trends in biodiversity. *Science advances*, 3, p.e1700315.

730 Hiddink, J.G., & Ter Hofstede, R., 2008. Climate induced increase in species richness of marine fishes.  
731 *Global Change Biology*, 13, 453-460.

732 Hilbe, J.M., 2011. *Negative Binomial Regression*. 2<sup>nd</sup> ed. Cambridge University Press, 553pp.

733 Hillebrand, H., 2004. Strength, slope and variability of marine latitudinal gradients. *Marine Ecology*  
734 *Progress Series*, 273, 251-267.

735 Hubbell, S.P., 2001. *The unified neutral theory of biodiversity and biogeography*. Monographs in  
736 Population Biology, Vol. 32. Princeton University Press. 375pp.

737 Jabot, F., & Chave, J., 2011. Analyzing tropical forest tree species abundance distributions using a  
738 non-neutral model and through approximate Bayesian inference. *The American Naturalist*, 178,  
739 E37-E47.

740 Jones, M.C., & Cheung, W.W.L., 2015. Multi-model ensemble projections of climate change effects  
741 on global marine biodiversity, *ICES Journal of Marine Science*, 72,741–752.

742 Kristensen, K., Nielsen, A., Berg, C.W., Skaug, H., & Bell, B., 2015. TMB: automatic differentiation and  
743 Laplace approximation. *arXiv preprint arXiv:1509.00660*.

744 Leis, J.M., Caselle, J.E., Bradbury, I.R., Kristiansen, T., Llopiz, J.K., Miller, M.J., ... Swearer, S.E., 2013.  
745 Does fish larval dispersal differ between high and low latitudes? *Proceedings of the Royal*  
746 *Society of London B: Biological Sciences*, 280, p.20130327.

747 Locarnini, R. A., Mishonov, A. V., Antonov, J. I., Boyer, T. P., Garcia, H. E., Baranova, ... Seidov, D.,  
748 2013. World Ocean Atlas 2013, Volume 1: Temperature. S. Levitus, Ed., A. Mishonov Technical  
749 Ed.; NOAA Atlas NESDIS 73, 40pp.

750 Macpherson, E., & Duarte, C. M., 1994. Patterns in species richness, size, and latitudinal range of  
751 East Atlantic fishes. *Ecography*, 17, 242-248.

752 Marbà, N., Jordà, G., Agustí, S., Girard, C., & Duarte, C.M., 2015. Footprints of climate change on  
753 Mediterranean Sea biota. *Frontiers in Marine Science*, 2:56 doi: 10.3389/fmars.2015.00056.

754 Meissa, B., & Gascuel, D., 2014. Overfishing of marine resources: some lessons from the assessment  
755 of demersal stocks off Mauritania. *ICES Journal of Marine Science*, 72, 414-427.

756 Mora, C., Tittensor, D.P., & Myers, R.A., 2008. The completeness of taxonomic inventories for  
757 describing the global diversity and distribution of marine fishes. *Proceedings of the Royal*  
758 *Society of London B: Biological Sciences*, 275, 149-155.

759 Oksanen, J., Blanchet, F.G., Friendly, M., Kindt, R., Legendre, P., ... Wagner, H., 2019. Vegan:  
760 Community Ecology Package. R package version 2.2-1.

761 Perry, A.L., Low, P.J., Ellis, J.R., & Reynolds, J.D., 2005. Climate change and distribution shifts in  
762 marine fishes. *Science*, 308, 1912–1915.

763 Pilson, M.E., & Seitzinger, S.P., 1996. Areas of shallow water in the North Atlantic. *Biogeochemistry*,  
764 35, 227-233.

765 Purvis, A., Orme, C.D.L., & Dolphin, K., 2003. *Why are Most Species Small-Bodied?* Macroecology:  
766 Concepts and Consequences, pp.155–173. Oxford University Press, Oxford.

767 Rabosky, D.L., Chang, J., Title, P.O., Cowman, P.F., Sallan, L., Friedman, ... Alfaro, M.E., 2018. An  
768 inverse latitudinal gradient in speciation rate for marine fishes. *Nature*, 55, 392–395

769 Reuman, D.C., Gislason, H., Barnes, C., Mélin, F., & Jennings, S., 2014. The marine diversity  
770 spectrum. *Journal of Animal Ecology*, 83, 963-979.

771 Romano, C., Koot, M.B., Kogan, I., Brayard, A., Minikh, A.V., Brinkmann, W., ... Kriwet, J., 2016.  
772 Permian–Triassic Osteichthyes (bony fishes): diversity dynamics and body size evolution.  
773 *Biological Reviews*, 91, 106-147.

774 Rosindell, J., Harmon, L.J., & Etienne, R.S., 2015. Unifying ecology and macroevolution with  
775 individual-based theory. *Ecology Letters*, 18, 472-482.

776 Rosindell, J., Hubbell, S.P., & Etienne, R.S., 2011. The unified neutral theory of biodiversity and  
777 biogeography at age ten. *Trends in Ecology and Evolution*, 26, 340-348.

778 Roy, K., Jablonski, D., & Martien, K.K., 2000. Invariant size-frequency distributions along a latitudinal  
779 gradient in marine bivalves. *Proc. Nat. Acad. Sci.*, 97, 13150–13155.

780 Rypel, A.L., 2013. The cold-water connection: Bergmann’s rule in North American freshwater fishes.  
781 *The American Naturalist*, 183, 147-156.

782 Segura, A.M., Calliari, D., Kruk, C., Fort, H., Izaguirre, I., Saad, J.F., & Arim, M., 2015. Metabolic  
783 dependence of phytoplankton species richness. *Global Ecology and Biogeography*, 24, 472-482.

784 Siemann, E., Tilman, D., & Haarstad, J., 1996. Insect species diversity, abundance and body size  
785 relationships. *Nature*, 380, 704-706.

786 Smith, F.A., & Lyons S.K., 2013. *Animal Body Size: Linking Pattern and Process across Space, Time,*  
787 *and Taxonomic Group.* University of Chicago Press. 272pp.

788 Storch, D., Bodhalkvá, E., & Okie, J., 2018. The more-individuals hypothesis revisited: the role of  
789 community abundance in species richness regulation and the productivity-diversity  
790 relationship. *Ecology Letters*, 21, 920-937.

791 Tittensor, D.P., Mora, C., Jetz, W., Lotze, H. K., Ricard, D., Berghe, E. V., & Worm, B., 2010. Global  
792 patterns and predictors of marine biodiversity across taxa. *Nature*, 466, 1098-1101.

793 Tittensor, D.P. & Worm, B., 2016. A neutral-metabolic theory of latitudinal biodiversity. *Global*  
794 *Ecology and Biogeography*, 25, 630-641.

795 Walker, N. D., Maxwell, D. L., Le Quesne, W. J., & Jennings, S., 2017. Estimating efficiency of survey  
796 and commercial trawl gears from comparisons of catch-ratios. *ICES Journal of Marine Science*,  
797 74, 1448-1457.

798 Wood, S.N., 2006. *Generalized additive models: an introduction with R.* Boca Raton, Florida:  
799 Chapman and Hall/CRC. 391pp.

800 Worm, B., & Tittensor, D.P., 2018. *A Theory of Global Biodiversity.* Monographs in Population  
801 Biology 60. Princeton University Press, 214 pp.

802 Wright, S.D., Ross, H.A., Keeling, D.J., McBride, P., & Gillman, L.N., 2011. Thermal energy and the  
803 rate of genetic evolution in marine fishes. *Evolutionary Ecology*, 25, 525-530.

804

805

806

807

808 Data accessibility

809 The richness and abundance data and the R-code that support the findings of this study are deposited

810 on GitHub (<https://github.com>) in the repository 'DTUAqua/biodiversity'.

811

812

813 Appendix 1 – Data Sources

814

815 Anon., 2006. Methodic manual on instrumental surveys of commercial hydrobiont stocks in PINRO  
816 investigations areas. Murmansk, PINRO Press, 163 pp. (in Russian).

817 Benchoucha, S., Berraho, A., Bazairi, H., Katara, I., Benchrifi, S., & Valavanis, V.D., 2008. Salinity and  
818 temperature as factors controlling the spawning and catch of *Parapenaeus longirostris* along  
819 the Moroccan Atlantic Ocean. *Hydrobiologia*, 612: 109-123.

820 Bertrand, J.A., Gil de Sola, L., Papaconstantinou, C., Relini, G., & Souplet, A., 2002. The general  
821 specification of the MEDITS surveys. *Scientia Marina* 66 (Suppl. 2), 9 -17.

822 Bourdages H., & Oullet, S., 2011. Geographic distribution and abundance indices of marine fish in  
823 the northern Gulf of St. Lawrence (1990-2009). *Can. Tech. Rep. Fish. & Aquat. Sci.* 2964.

824 Domain, F., Chavance, P., & Diallo, A., (éds.), 1999. La pêche côtière en Guinée : ressources et  
825 exploitation. IRD édition, Paris, *Collection colloques et séminaires*, 394 p.

826 Fowler, G.M., & and Showell, M.A., 2009. Calibration of bottom trawl survey vessels: comparative  
827 fishing between the Alfred Needler and Teleost on the Scotian Shelf during the summer of  
828 2005. *Can. Tech. Rep. Fish. Aquat. Sci.* 2824: iv + 25 p.

829 Gascuel, D., Labrosse, P., Meissa, B., Taleb Sidi, M.O., & Guénette, S., 2007. Decline of the demersal  
830 resources in the North-West Africa: an analysis of Mauritanian trawl-survey data over the past  
831 25 years. *African Journal of Marine Science*, 29: 331-345.

832 ICES 2017. Manual of the IBTS North Eastern Atlantic Surveys. Series of ICES Survey Protocols SISP  
833 15. 92 pp. <http://doi.org/10.17895/ices.pub.3519>

834 Jørgensen O.A., 1998. Survey for Greenland Halibut in NAFO Division 1C-1D. *NAFO Sci. Council*  
835 *Reports*. Doc. 98/25. Serial No. N3010, 26 pp.

836 Magnussen, E., 2002. Demersal fish assemblages of Faroe Bank: species composition, distribution,  
837 biomass spectrum and diversity. *Marine Ecology Progress Series*, 238, 211-225.

838 Marine Research Institute, 2010. Manuals for the Icelandic bottom trawl surveys in spring and  
839 autumn. Marine Research in Iceland: 125 pp.

840 <https://www.hafogvatn.is/static/research/files/fjolrit-156.pdf>

841 Rätz, H-J., 1999, Structures and Changes of the Demersal Fish Assemblage off Greenland, 1982-96.  
842 *NAFO Sci. Council Studies*, 32: 1-15.

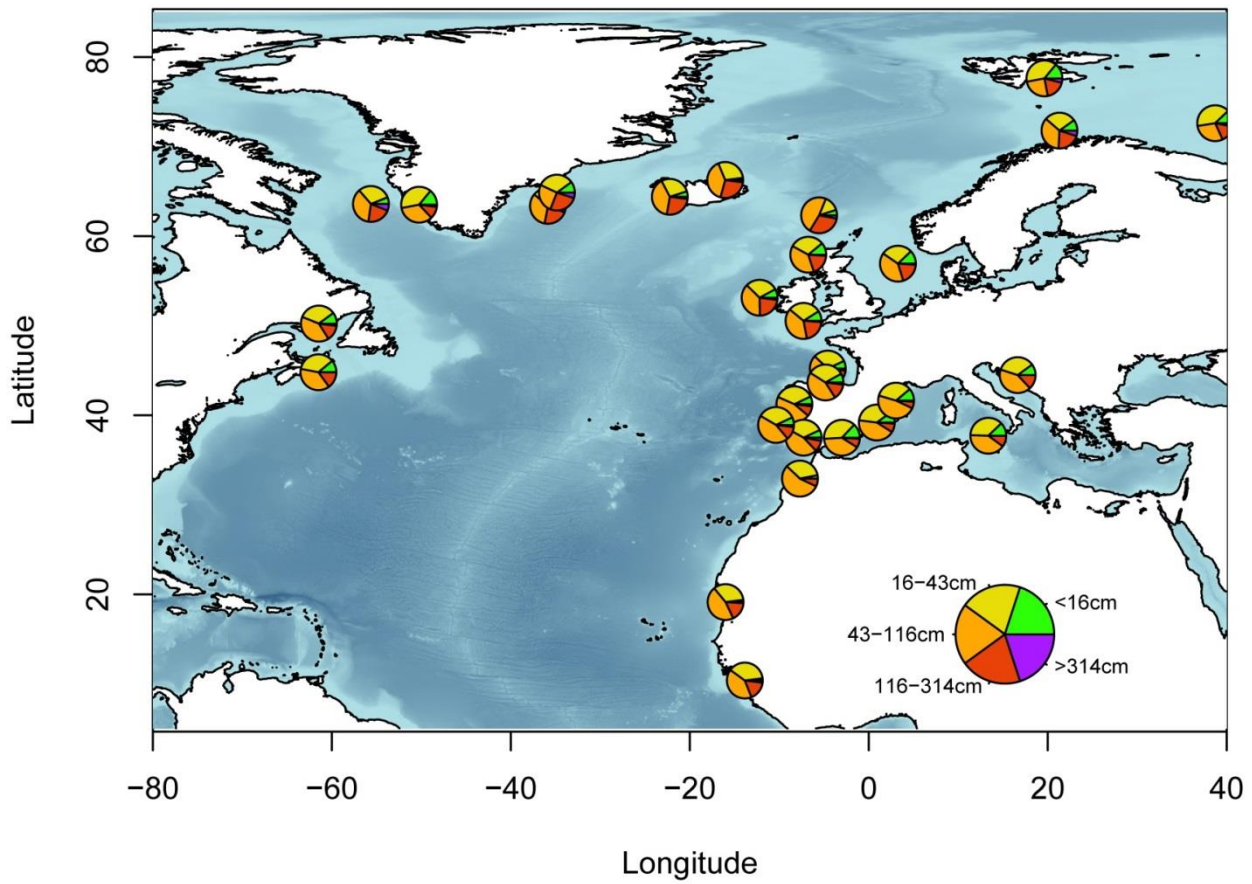
843

844 Table 1. Parameter estimates from TMB-model fits using average absolute density and abundance.  
 845 Standard error in parentheses and significance levels indicated by stars (\*\*= $<0.001$ , \*\*= $<0.01$ , \*= $<$   
 846  $0.05$ ) (one-sided t-test,  $n=550$ ). NS= Non Significant term retained in the model fit. NSR= Non  
 847 Significant term removed from the model.

Parameter		Best descriptive model	Neutral	Metabolic	Environmental
Constant	$(\log\alpha)$	16.90 (1.63)***	22.95 (1.35)***	24.89 (1.65)***	3.093 (0.687)***
Latitude	$(\beta_0)$				-0.518 (0.055)***
Longitude	$(\beta_1)$				0.426 (0.073)***
Temperature	$(\beta_2)$	0.322 (0.035)***	0.521 (0.029)***	0.466 (0.029)***	
Abundance	$(\beta_3)$	0.034 (0.009)***			
Density	$(\beta_3)$			0.056 (0.011)***	
Depth	$(\beta_4)$	-0.115 (0.029)***			-0.167 (0.034)***
Net prim. prod.	$(\beta_5)$	0.217 (0.045)***			
Max. length	$(\beta_6)$			-1.000 (0.246)***	
Log. max. length <sup>2</sup>	$(\beta_7)$	-0.131 (0.028)***	-0.131 (0.031)***		-0.235 (0.029)***
Immigration	$(\lambda)$		NS		
Catch	$(\beta_8)$	NSR	NSR	NSR	0.067 (0.010)***
Area swept	$(\beta_9)$	0.079 (0.023)***	0.129 (0.022)***	0.176 (0.022)***	NSR
Mesh:mlgr <sub>1.5</sub>	$(\beta_{11,1})$	-1.537 (0.181)***	-1.351 (0.184)***	-1.675 (0.242)***	-1.070 (0.187)***
Mesh:mlgr <sub>2.0</sub>	$(\beta_{11,2})$	-1.378 (0.162)***	-1.205 (0.164)***	-1.421 (0.202)***	-1.021 (0.168)***
Mesh:mlgr <sub>2.5</sub>	$(\beta_{11,3})$	-0.977 (0.120)***	-0.875 (0.124)***	-0.972 (0.143)***	-0.755 (0.125)***
Mesh:mlgr <sub>3.0</sub>	$(\beta_{11,4})$	-0.598 (0.099)***	-0.509 (0.103)***	-0.552 (0.108)***	-0.458 (0.103)***
Mesh:mlgr <sub>3.5</sub>	$(\beta_{11,5})$	-0.401 (0.078)***	-0.335 (0.081)***	-0.347 (0.082)***	-0.340 (0.082)***
Mesh:mlgr <sub>4.0</sub>	$(\beta_{11,6})$	-0.222 (0.066)***	-0.165 (0.070)**	-0.167 (0.070)*	-0.192 (0.070)***
Mesh:mlgr <sub>4.5</sub>	$(\beta_{11,7})$	NS	NS	NS	NS
Mesh:mlgr <sub>5.0</sub>	$(\beta_{11,8})$	NS	NS	NS	NS
Mesh:mlgr <sub>5.5</sub>	$(\beta_{11,9})$	NS	NS	NS	NS
Mesh:mlgr <sub>6.0</sub>	$(\beta_{11,10})$	NS	NS	NS	NS
Mesh:mlgr <sub>6.5</sub>	$(\beta_{11,11})$	NS	NS	NS	NS
Scale parameter	$(\log\kappa)$	3.752 (0.402)***	3.058 (0.239)***	3.085 (0.247)***	3.049 (0.239)***
Proportion of deviance explained		0.900	0.892	0.891	0.890
Pearson's R <sup>2</sup> (observed vs. predicted)		0.838	0.787	0.792	0.789
AIC		1891	1929	1931	1937
$\Delta$ AIC			38	40	46

848

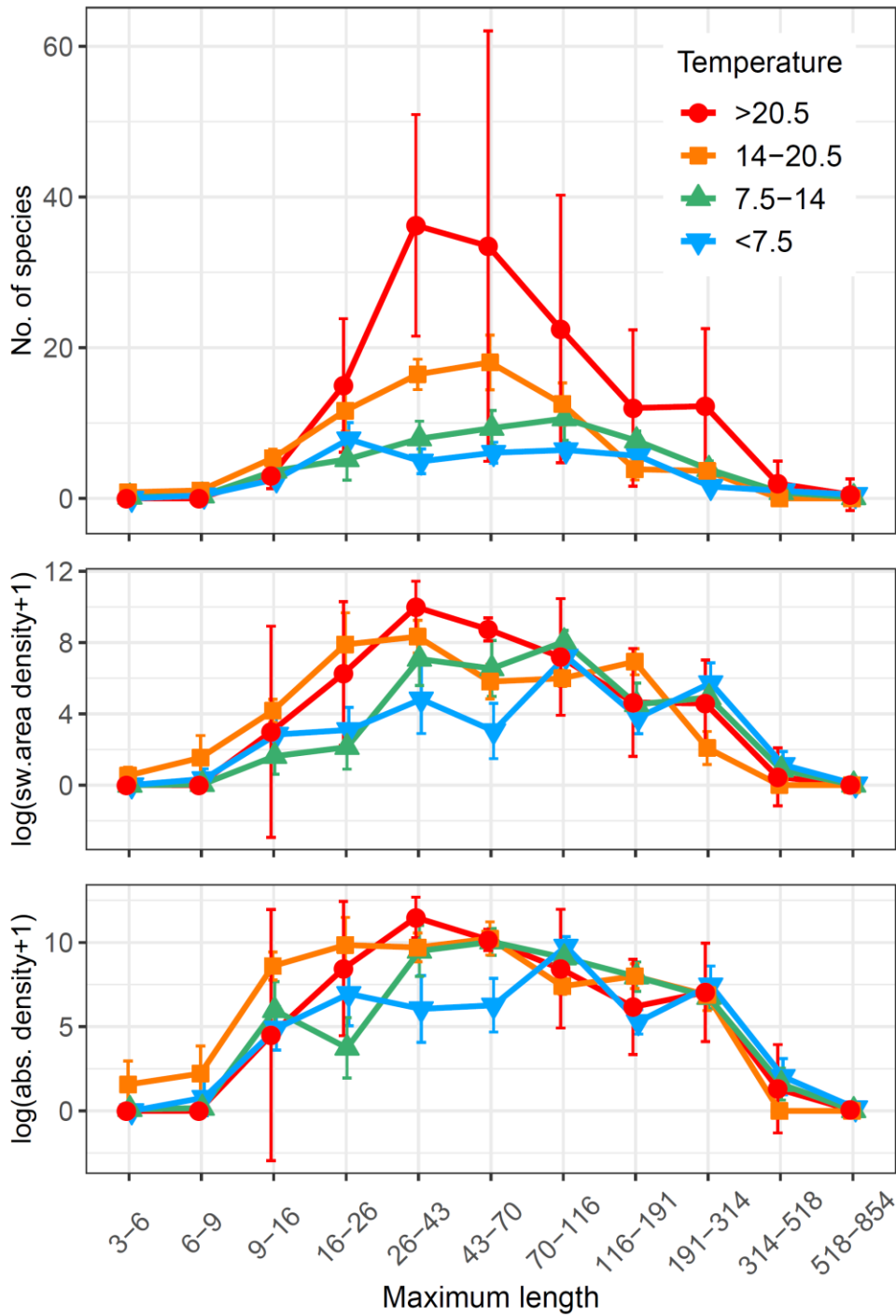
849



850

851 Figure 1. Pies showing the locations of the surveys and the relative number of species recorded in  
852 each of the maximum length groups indicated in the lower right-hand corner of the map (plotted with  
853 the R-package 'marmap').

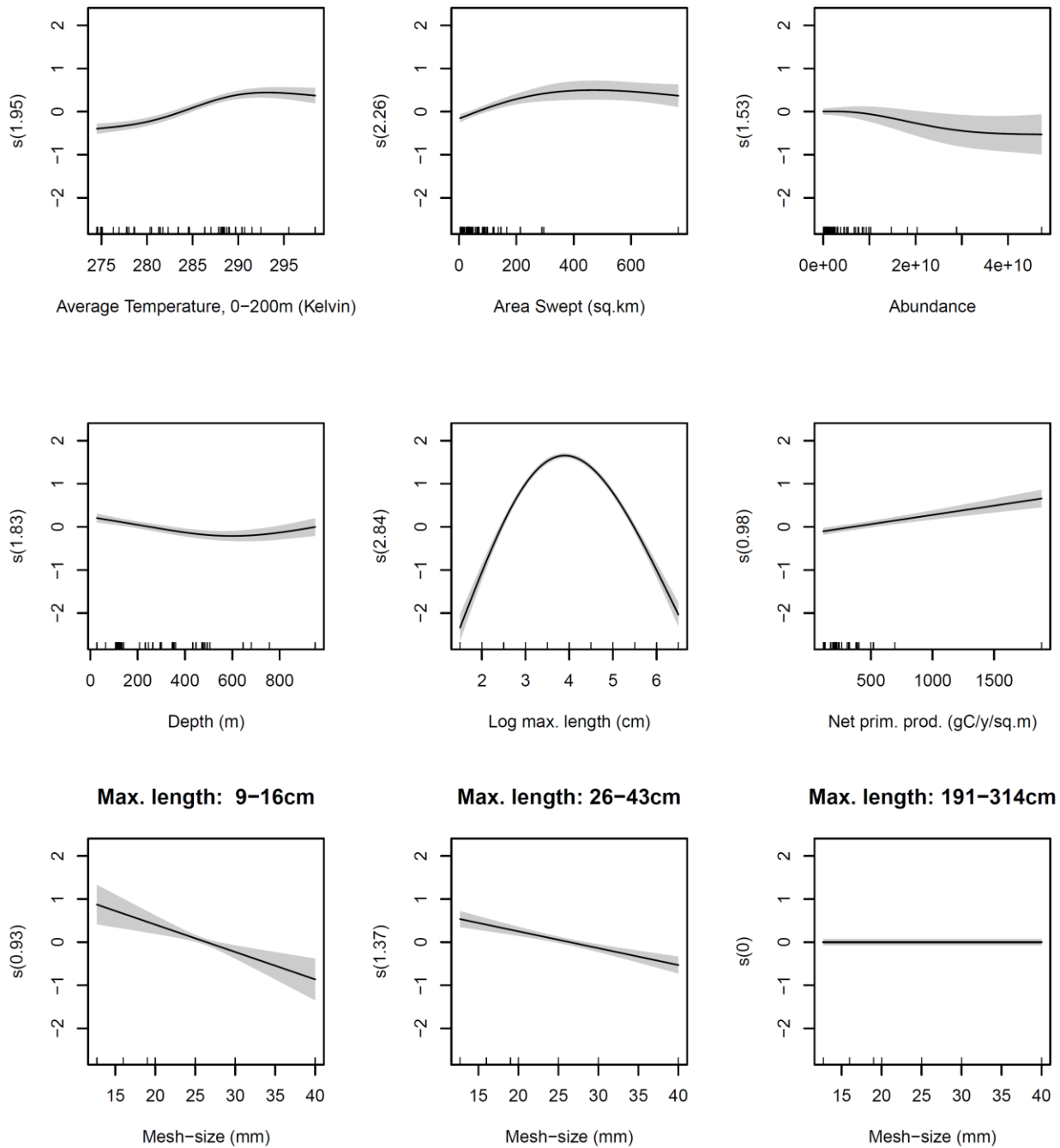
854



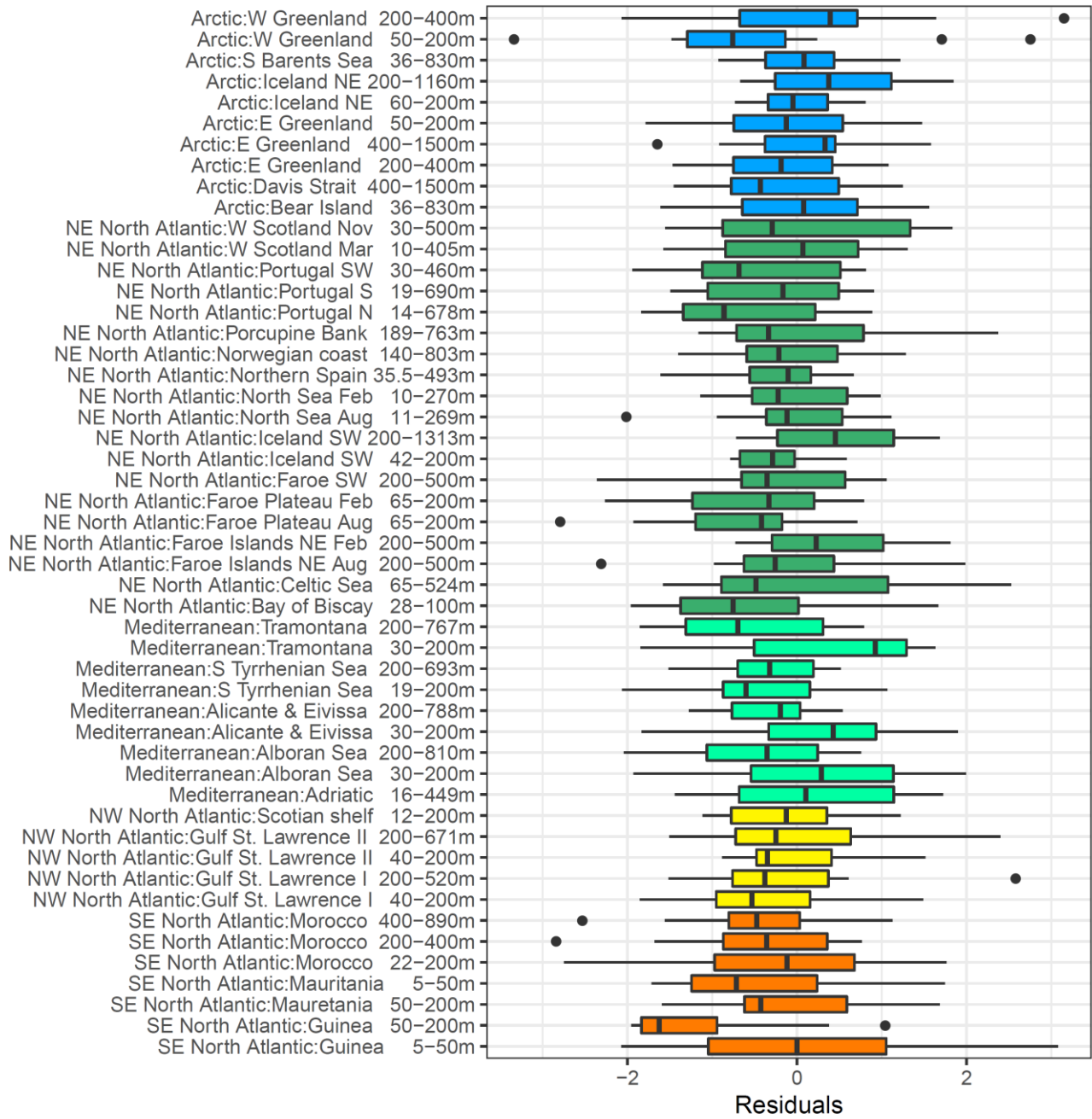
855

856 Figure 2. Average number of species, log swept area density (No\*km<sup>-2</sup>) and log absolute density  
 857 (No\*km<sup>-2</sup>) (±95% conf. limits) versus maximum length (cm) in four different sea surface temperature  
 858 intervals (°C).

859 Figure 3. Estimated smoothing curves from the GAM using average sea temperature and other  
 860 covariates to model the number of species observed by log maximum length group. Estimated  
 861 degrees of freedom in brackets on the y-axis labels. Shaded area: 2\*SE. Mesh-size smooths in bottom  
 862 row only shown for three numerically abundant maximum length groups.



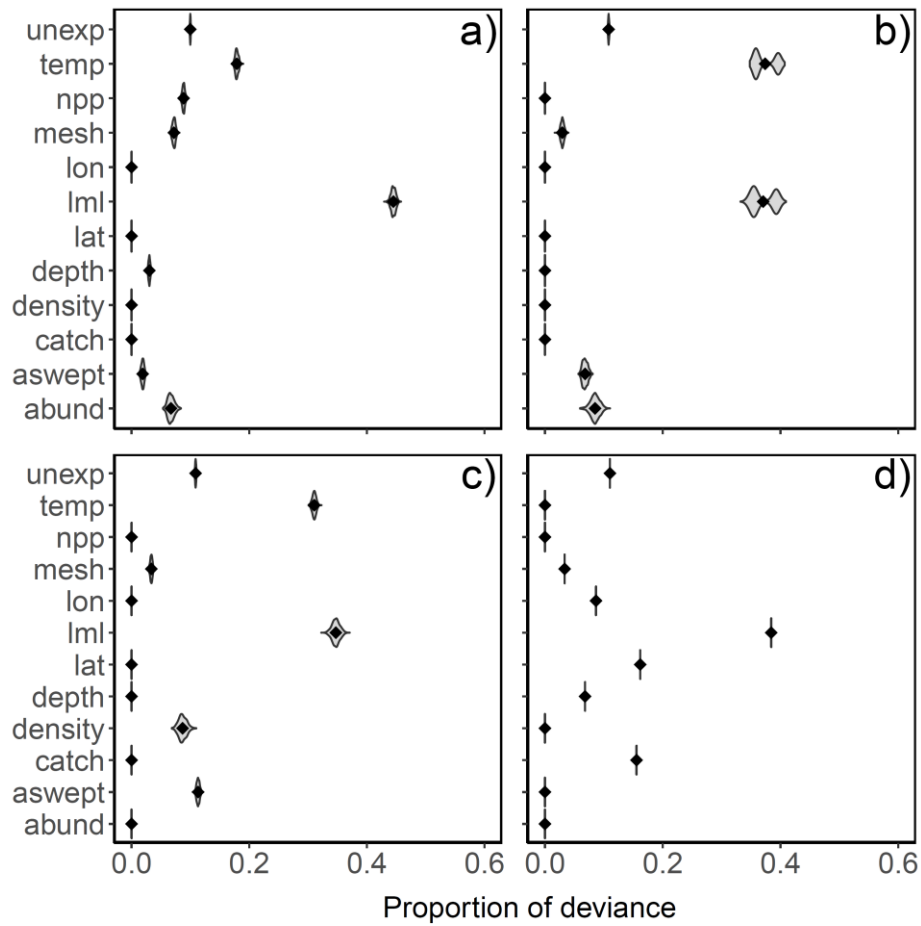
863



865

866 Figure 4. Box and whisker plot of log survey strata residuals from GAM model (box limits show 25%  
 867 and 75% quartiles; the vertical bar in the middle of the box is the median of the residuals; whiskers  
 868 show max. and min. values; and black dots are outliers; colour indicate geographic regions).

869



870

871

872 Figure 5. Violin plots of the relative contribution of the variables in each of the four models to the total  
 873 deviance explained by each model. Results from 1000 non-linear model runs with stochastic  
 874 catchabilities. Unexplained deviance: unexp. Models: a) 'best' descriptive, b) neutral, c) metabolic, d)  
 875 environmental.